

AN OPTIMIZATION PERSPECTIVE ON WINTER'S ENDMEMBER EXTRACTION BELIEF

Tsung-Han Chan[†], Wing-Kin Ma^{*}, ArulMurugan Ambikapathi[†], and Chong-Yung Chi[†]

[†]Inst. Communications Eng. & Dept. Electrical Eng., National Tsing Hua Univ., Hsinchu, Taiwan

^{*}Dept. Electronic Eng., Chinese Univ. of Hong Kong, Shatin, N.T., Hong Kong

E-mail: {thchan, wkma, aareul}@ieee.org; cychi@ee.nthu.edu.tw

ABSTRACT

In this paper, we describe a continuous optimization perspective on Winter's simplex volume maximization belief for endmember extraction in hyperspectral remote sensing. Winter's belief, proposed in the late 90's, is very insightful and has led to one of the most widely used class of endmember extraction algorithms nowadays—N-FINDR. Our endeavor to revisit this problem is to provide an alternative, systematic, framework of formulating and understanding Winter's belief. Under the continuous optimization formulation of Winter's belief, we show a fundamental result that the existence of pure pixels is not only sufficient for the Winter problem to perfectly identify the ground-truth endmembers, but also necessary. Then, we derive two Winter-based algorithms based on two different optimization strategies. Interestingly, the resulting algorithms are found to be similar to an N-FINDR variant and the vertex component analysis (VCA) algorithm. Hence, the developed framework provides linkage and alternative interpretations to these existing algorithms. Simulation results are also presented to compare the derived Winter algorithms and several existing algorithms.

Index Terms— Endmember extraction, Simplex volume maximization, Alternating optimization, Successive optimization

1. INTRODUCTION

In space object exploration in cosmos [1], as well as environmental and military monitoring on the Earth [2], using a hyperspectral sensor, endmember extraction techniques are essential to identifying the composition of disparate materials over the observed scene. How to design an effective endmember extraction algorithm has therefore been a subject of numerous investigations during the past decade [3]. One major group of endmember extraction algorithms [4–6] is based on Craig's belief [7], which states that the vertices of a minimum-volume simplex enclosing all the observed pixel vectors may serve as reliable estimates of the endmembers. However, algorithms based on Craig's belief can be expensive to implement, owing to the complexity required to handle pixel enclosing simplexes. Another group of endmember extraction algorithms, which are generally simpler to implement, assumes the existence of pure pixels and attempts to search for those pure pixels as endmember estimates. The idea started in the later 90's, when Winter proposed a belief that among all pixel-constructed simplexes, the one formed by the pure pixels should yield the maximum simplex volume [8]. From this very insightful belief he then suggested a way to practically extract endmembers, well known as N-finder (N-FINDR). The working principle of N-FINDR is to exhaustively examine each pixel and recalculate the corresponding simplex volume until it reaches the maximum.

This work is supported by a General Research Fund of Hong Kong Research Grant Council (Project No. CUHK415509), and by the National Science Council (R.O.C.) under Grant NSC 99-2221-E-007-003-MY3.

Winter's idea has stimulated much interest, leading to many different N-FINDR implementations being proposed recently [9].

In this paper, we adopt a different view to study Winter's belief, where our objective is to provide new insights and interpretations of the Winter approach. Specifically, we take a continuous optimization perspective to revisit Winter's belief. By establishing a continuous Winter problem formulation and then studying it, some interesting results are obtained. The first is regarding the fundamental limitation. In [10], we have proven that theoretically, the Winter problem can indeed lead to exact identification of the true endmembers under the pure-pixel assumption. Here, we will show that the existence of pure pixels is also necessary for the Winter problem to perfectly identify the true endmembers. The latter gives a key implication—the Winter-based endmember extraction algorithms would be most suitable for the pure-pixel existent scenario.

Despite the fundamental limitation described above, Winter-based algorithms are attractive owing to their relatively simple algorithmic structures. The second result arising from our continuous optimization perspective is on the algorithm aspect. Instead of following the path of N-FINDR, we consider continuous optimization strategies for dealing with the Winter problem. Specifically, we propose to apply an alternating optimization strategy and a successive optimization strategy to the Winter problem. Interestingly, the resulting optimization algorithms turn out to be similar to N-FINDR and vertex component analysis (VCA) [11] in an algorithmic way. Although our derived Winter optimization algorithms still have some algorithmic differences in comparison to N-FINDR and VCA, the similarities shed new light on N-FINDR and VCA from an optimization perspective. Some simulations are presented to compare our derived Winter-based algorithms and several existing algorithms.

Notations: \succeq denotes componentwise inequality, $\|\cdot\|_2$ is the Euclidean norm; $\mathbf{1}_N$ and \mathbf{e}_i represent the $N \times 1$ all-one vector and the unit vector with the i th entry equal to 1, respectively; $[\mathbf{x}]_i$ denotes the i th element of \mathbf{x} , and \mathbf{X}^\dagger denotes the pseudo inverse of \mathbf{X} .

2. WINTER'S ENDMEMBER EXTRACTION PROBLEM

Assuming that the incident solar radiation gets reflected from the Earth surface through a single bounce and the materials are distinct [3–11], each pixel vector of the hyperspectral data cube can be represented by the following linear mixing model:

$$\mathbf{x}[n] = \mathbf{A}\mathbf{s}[n] = \sum_{i=1}^N s_i[n]\mathbf{a}_i, \quad n = 1, \dots, L, \quad (1)$$

where $\mathbf{x}[n] = [x_1[n], \dots, x_M[n]]^T$ is the n th observed pixel vector comprising M spectral bands, $\mathbf{A} = [\mathbf{a}_1, \dots, \mathbf{a}_N] \in \mathbb{R}^{M \times N}$ denotes the signature matrix whose i th column vector \mathbf{a}_i is the i th endmember signature, $\mathbf{s}[n] = [s_1[n], \dots, s_N[n]]^T$ is the corresponding abundance vector comprising N fractional abundances, and L is the total number of observed pixel vectors.

The endmember extraction problem is to estimate \mathbf{A} from the

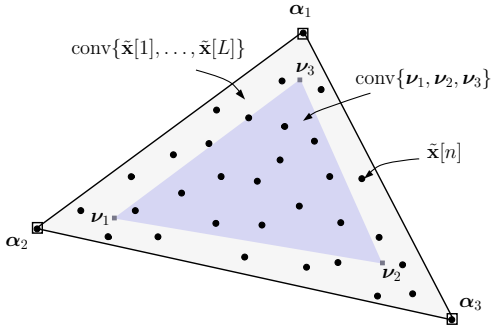


Fig. 1. An example of signal geometry of Winter's belief for $N = 3$.

observed pixel vectors $\mathbf{x}[n]$, given prior knowledge of N . Some general assumptions are as follows: (A1) $s_i[n] \geq 0$ for all i and n ; (A2) $\sum_{i=1}^N s_i[n] = 1$ for all n ; (A3) $\min\{L, M\} \geq N$ and $\mathbf{a}_1, \dots, \mathbf{a}_N$ are linearly independent; (A4) there exist pure pixels, i.e., $\mathbf{x}[\ell_i] = \mathbf{a}_i$, $i = 1, \dots, N$ for some index set $\{\ell_1, \dots, \ell_N\}$.

We employ a dimension reduction process based on convex geometry (see [6] for the details), given as follows:

$$\tilde{\mathbf{x}}[n] \triangleq \mathbf{C}^T(\mathbf{x}[n] - \mathbf{d}) = \sum_{i=1}^N s_i[n] \alpha_i \in \mathbb{R}^{N-1}, \quad n = 1, \dots, L, \quad (2)$$

where $\alpha_i = \mathbf{C}^T(\mathbf{a}_i - \mathbf{d}) \in \mathbb{R}^{N-1}$, $i = 1, \dots, N$, are dimension reduced endmembers, $\mathbf{d} = \frac{1}{L} \sum_{n=1}^L \mathbf{x}[n]$ and $\mathbf{C} = [\mathbf{q}_1(\mathbf{H}\mathbf{H}^T), \dots, \mathbf{q}_{N-1}(\mathbf{H}\mathbf{H}^T)]$ in which $\mathbf{H} = [\mathbf{x}[1] - \mathbf{d}, \dots, \mathbf{x}[L] - \mathbf{d}] \in \mathbb{R}^{M \times L}$ and $\mathbf{q}_i(\mathbf{H}\mathbf{H}^T)$ denotes the unit-norm eigenvector associated with the i th principal eigenvalue of $\mathbf{H}\mathbf{H}^T$. The same linear mixing model as in (1) is still preserved in (2); however, the dimension of $\tilde{\mathbf{x}}[n]$ is $N - 1$, which is much less than that of $\mathbf{x}[n]$.

As mentioned in Section 1, Winter's belief states that the true endmembers may be obtained by finding a collection of pixel vectors whose simplex volume is the largest [8]. Following Winter's belief and (2), we formulate Winter's endmember extraction problem in form of continuous optimization as follows [10]:

$$\begin{aligned} \max_{\nu_1, \dots, \nu_N \in \mathbb{R}^{N-1}} & |\det(\Delta(\nu_1, \dots, \nu_N))| \\ \text{s.t.} & \nu_i \in \mathcal{F}, \quad i = 1, \dots, N, \end{aligned} \quad (3)$$

where $\mathcal{F} = \{\nu \in \mathbb{R}^{N-1} \mid \nu = \tilde{\mathbf{X}}\theta, \theta \succeq \mathbf{0}, \mathbf{1}_L^T \theta = 1\}$ is the convex hull of $\tilde{\mathbf{x}}[1], \dots, \tilde{\mathbf{x}}[L]$, $\tilde{\mathbf{X}} = [\tilde{\mathbf{x}}[1], \dots, \tilde{\mathbf{x}}[L]]$, and

$$\Delta(\nu_1, \dots, \nu_N) = \begin{bmatrix} \nu_1 & \cdots & \nu_N \\ 1 & \cdots & 1 \end{bmatrix} \in \mathbb{R}^{N \times N}. \quad (4)$$

We name Problem (3) the *Winter problem* in the sequel. The Winter problem aims to find an N -tuple (ν_1, \dots, ν_N) from the pixel-constructed convex hull such that the associated simplex volume is maximum. A picture is used to illustrate this in Figure 1. It should be noted that in Winter's original work [8], each endmember estimate ν_j is restricted to be any dimension-reduced pixel vector in $\{\tilde{\mathbf{x}}[1], \dots, \tilde{\mathbf{x}}[L]\}$, rather than the continuous set \mathcal{F} in (3).

In Appendix 5.1, we prove the endmember identifiability of Winter's belief as stated in the following theorem:

Theorem 1. (Endmember identifiability for Winter's belief)

Suppose that noise is absent, and that (A1) – (A3) hold. Then, the optimal solution of (3), denoted by $\{\nu_1^*, \dots, \nu_N^*\}$, is uniquely given by $\{\alpha_1, \dots, \alpha_N\}$ if and only if (A4) holds.

The implications of Theorem 1 are twofold. First, for the pure-pixel existent case, solving the Winter problem can lead to perfect identification, or error-free extraction, of all the true endmembers [10].

Second, such perfect identification would not be possible in the absence of pure pixels. The latter implies that in the absence of pure pixels, a Winter-based endmember extraction algorithm would be subject to estimation errors even without noise effects.

Despite the limitation described above, the Winter approach provides an attractive option to endmember extraction. In practice, it is expected that if the pure-pixel condition is too seriously violated, the estimation errors caused by lack of pure pixels should be small. More importantly, the Winter problem (3) has a good problem structure that one can exploit to develop simple, efficient, endmember extraction algorithms. The latter will be explored in the next section.

3. OPTIMIZATION OF THE WINTER PROBLEM

In the two subsequent subsections, we will introduce two different optimization strategies for handling the Winter problem (3).

3.1. ALTERNATING VOLUME MAXIMIZATION (AVMAX)

Alternating optimization, also known as block coordinate descent/ascent and nonlinear Gauss-Seidel, is a pragmatic approach to handling certain classes of difficult optimization problems [12]. Before proceeding to describing its application to the Winter problem, let us consider a simplified form of problem (3), given as follows:

$$\max_{\nu_i \in \mathcal{F}, i=1, \dots, N} \det(\Delta(\nu_1, \dots, \nu_N)) \quad (5)$$

where we have removed the absolute function from the objective function. It is shown [13] that problems (5) and (3) are equivalent. To optimize problem (5) with respect to all endmember estimates ν_1, \dots, ν_N jointly can be difficult, due to the nonconvexity of determinant. In alternating optimization, we employ a divide and conquer rationale—maximize the objective function of (5) over one ν_i at a time, while holding the others fixed. We can represent this by

$$\hat{\nu}_j := \arg \max_{\nu_j \in \mathcal{F}} \det(\Delta(\hat{\nu}_1, \dots, \hat{\nu}_{j-1}, \nu_j, \hat{\nu}_{j+1}, \dots, \hat{\nu}_N)), \quad \forall j \quad (6)$$

where $(\hat{\nu}_1, \dots, \hat{\nu}_N)$ denotes the alternatingly optimized endmember iterates. Note that the partial maximization in (6) is conducted in a cyclic manner until some stopping rule is met.

Alternating optimization is attractive in that it shows a neat closed-form solution to each partial maximizer (6). By applying cofactor expansion to $\det(\Delta(\nu_1, \dots, \nu_N))$, each partial maximizer (6) can be written as

$$\hat{\nu}_j := \arg \max_{\nu_j \in \mathcal{F}} \mathbf{b}_j^T \nu_j + (-1)^{N+j} \det(\mathbf{V}_{Nj}), \quad (7)$$

where $\mathbf{b}_j = [(-1)^{i+j} \det(\mathbf{V}_{ij})]_{i=1}^{N-1} \in \mathbb{R}^{N-1}$, and $\mathbf{V}_{ij} \in \mathbb{R}^{(N-1) \times (N-1)}$ is a submatrix of $\Delta(\hat{\nu}_1, \dots, \hat{\nu}_N)$ with the i th row and j th column removed. It can be shown that problem (7) has a closed-form solution, as stated in the following lemma

Lemma 1. Consider the j th partial maximization problem (7). Let

$$\mathcal{I}_j = \left\{ \ell \in \{1, \dots, L\} \mid \mathbf{b}_j^T \tilde{\mathbf{x}}[\ell] = \max_{n=1, \dots, L} \mathbf{b}_j^T \tilde{\mathbf{x}}[n] \right\}. \quad (8)$$

A point $\hat{\nu}_j$ is optimal to (7) if and only if it is a convex combination of $\{\tilde{\mathbf{x}}[n]\}_{n \in \mathcal{I}_j}$; i.e., any point $\hat{\nu}_j = \sum_{\ell \in \mathcal{I}_j} \beta_\ell \tilde{\mathbf{x}}[\ell]$ where $\sum_{\ell \in \mathcal{I}_j} \beta_\ell = 1$, $\beta_\ell \geq 0$ for all $\ell \in \mathcal{I}_j$, is an optimal solution to (7) and vice versa.

The proof of Lemma 2 is given in Appendix 5.2.

The resulting algorithm, which we call *alternating volume maximization (AVMAX)*, is summarized in Table 1. An important observation is that AVMAX algorithm is similar to the N-FINDR algorithms [8, 9] in terms of the algorithmic structures—the former and latter both attempt to maximize the simplex volume in some forms

of one-at-a-time pixel search. Among the variants of N-FINDR algorithms, AVMAX is particularly similar to the SC-N-FINDR algorithm [9]. To be specific, the pseudo code of AVMAX in Table 1 becomes that of SC-N-FINDR if we replace **S3** by $\hat{\mathbf{v}}_j = \tilde{\mathbf{x}}[\ell]$ for any $\ell = \arg \max_{n=1, \dots, L} |\det(\hat{\mathbf{v}}_1, \dots, \hat{\mathbf{v}}_{j-1}, \tilde{\mathbf{x}}[n], \hat{\mathbf{v}}_{j+1}, \dots, \hat{\mathbf{v}}_N)|$ and restrict the number of alternating cycles to one (i.e., enforces termination at $\kappa = 1$). From a different perspective, one may alternatively interpret SC-N-FINDR as an alternating optimization algorithm under the continuous Winter formulation.

3.2. SUCCESSIVE VOLUME MAXIMIZATION (SVMAX)

The second optimization strategy we propose for the Winter problem is successive optimization. Successive optimization is an approach that requires a specific decomposition structure of the objective function. To put into context, the Winter problem needs to be cast to a suitable form. By letting $\mathbf{w}_i = [\nu_i^T \ 1]^T$ and $\mathbf{W} = [\mathbf{w}_1, \dots, \mathbf{w}_N] \in \mathbb{R}^{N \times N}$, the Winter problem in (3) can be equivalently written as

$$\max_{\mathbf{w}_i \in \overline{\mathcal{F}}, i=1, \dots, N} |\det(\mathbf{W})|, \quad (9)$$

where $\overline{\mathcal{F}} = \{\mathbf{w} \in \mathbb{R}^N \mid \mathbf{w} = \overline{\mathbf{X}}\boldsymbol{\theta}, \boldsymbol{\theta} \succeq \mathbf{0}\}$, $\tilde{\mathbf{x}}[n] = [\tilde{\mathbf{x}}[n]^T \ 1]^T$ and $\overline{\mathbf{X}} = [\tilde{\mathbf{x}}[1], \dots, \tilde{\mathbf{x}}[L]]$. To facilitate the application of successive optimization to (9), we derive the following general matrix lemma:

Lemma 2. Let $\mathbf{Y} = [\mathbf{y}_1, \dots, \mathbf{y}_N] \in \mathbb{R}^{M \times N}$. It holds true that

$$\sqrt{\det(\mathbf{Y}^T \mathbf{Y})} = \|\mathbf{y}_1\|_2 \left\| \mathbf{P}_{\mathbf{Y}_{1:1}}^\perp \mathbf{y}_2 \right\|_2 \cdots \left\| \mathbf{P}_{\mathbf{Y}_{1:(N-1)}}^\perp \mathbf{y}_N \right\|_2, \quad (10)$$

where $\mathbf{Y}_{1:j} = [\mathbf{y}_1, \dots, \mathbf{y}_j]$, $\mathbf{P}_{\mathbf{Y}_{1:j}}^\perp = \mathbf{I}_M - \mathbf{Y}_{1:j}(\mathbf{Y}_{1:j}^T \mathbf{Y}_{1:j})^\dagger \mathbf{Y}_{1:j}^T$ is the orthogonal complement projector of $\mathbf{Y}_{1:j}$.

Lemma 2 is proven by Schur's formula and matrix analysis. We omit the proof due to the space limit, and its details will be given in [13]. Since $|\det(\mathbf{W})| = \sqrt{\det(\mathbf{W}^T \mathbf{W})}$, we can use Lemma 1 to decompose the objective function of Problem (9), thereby obtaining the following equivalent from:

$$\begin{aligned} \max_{\mathbf{w}_1, \dots, \mathbf{w}_N \in \mathbb{R}^N} f_1(\mathbf{w}_1) f_2(\mathbf{w}_1, \mathbf{w}_2) \cdots f_N(\mathbf{w}_1, \dots, \mathbf{w}_N) \\ \text{s.t. } \mathbf{w}_i \in \overline{\mathcal{F}}, i = 1, \dots, N. \end{aligned} \quad (11)$$

where

$$f_1(\mathbf{w}_1) = \|\mathbf{w}_1\|_2 \quad (12)$$

$$f_j(\mathbf{w}_1, \dots, \mathbf{w}_j) = \left\| \mathbf{P}_{\mathbf{W}_{1:(j-1)}}^\perp \mathbf{w}_j \right\|_2, \quad j = 2, \dots, N. \quad (13)$$

Now, we consider the successive optimization method. In this method, the endmembers are recursively estimated by

$$\hat{\mathbf{w}}_j = \arg \max_{\mathbf{w}_j \in \overline{\mathcal{F}}} f_j(\hat{\mathbf{w}}_1, \dots, \hat{\mathbf{w}}_{j-1}, \mathbf{w}_j), \quad (14)$$

from $j = 1$ to N . The j th endmember, \mathbf{w}_j , is determined by finding a maximizer of the decomposed sub-objective function $f_j(\hat{\mathbf{w}}_1, \dots, \hat{\mathbf{w}}_{j-1}, \mathbf{w}_j)$, fixing the previously determined endmembers $\hat{\mathbf{w}}_1, \dots, \hat{\mathbf{w}}_{j-1}$. The obtained partial maximizer $\hat{\mathbf{w}}_j$, together with the previous partial maximizers $\hat{\mathbf{w}}_1, \dots, \hat{\mathbf{w}}_{j-1}$, are then used to determine the next endmember. Notice that unlike alternating optimization, successive optimization is not an iterative method and requires no initial point to start with. Moreover, the partial maximization problems in (14) have simple solutions:

Lemma 3. For each j , the partial maximizer in (14) is given by $\hat{\mathbf{w}}_j = \tilde{\mathbf{x}}[\ell]$, where

$$\ell \in \begin{cases} \arg \max_{n=1, \dots, L} \|\tilde{\mathbf{x}}[n]\|_2, & j = 1 \\ \arg \max_{n=1, \dots, L} \left\| \mathbf{P}_{\mathbf{W}_{1:(j-1)}}^\perp \tilde{\mathbf{x}}[n] \right\|_2, & j > 1 \end{cases} \quad (15)$$

The proof of Lemma 3 is given in Appendix 5.3.

We name the successive optimization procedure developed above the *successive volume maximization (SVMAX)* algorithm. Table 1 also provides the pseudo code of the SVMAX algorithm. As another interesting coincidence, SVMAX appears to be similar to the VCA algorithm [11] in algorithmic structures. The notably similar part lies in the result in Lemma 3: If we replace the index selection in (15) by $\ell \in \arg \max_{n=1, \dots, L} |\mathbf{r}_j^T \tilde{\mathbf{x}}[n]|$, where $\mathbf{r}_j = \mathbf{P}_{\mathbf{W}_{1:(j-1)}}^\perp \boldsymbol{\xi} / \|\mathbf{P}_{\mathbf{W}_{1:(j-1)}}^\perp \boldsymbol{\xi}\|$ with $\boldsymbol{\xi}$ being randomly generated, the resulting algorithm would be similar to VCA. As one can see, both VCA and SVMAX employ some forms of orthogonal complement projections onto the previously determined $\hat{\mathbf{w}}_1, \dots, \hat{\mathbf{w}}_{j-1}$ at each stage, and they both do so in a successive manner.

4. SIMULATIONS AND CONCLUSION

Two Monte Carlo simulations of one hundred independent runs are presented to demonstrate the advantages of the proposed AVMAX and SVMAX algorithms. Three existing endmember extraction algorithms, SQ-N-FINDR [9], SC-N-FINDR [9], and VCA [11] were tested for comparison. In each run, we synthetically generated noisy hyperspectral data by 8 endmember signatures with 224 bands selected from the U.S. geological survey (USGS) library, abundances generated from Dirichlet distribution [11], and additive zero-mean white Gaussian noise based on the specified signal-to-noise ratio (SNR). The root-mean-square spectral angle distance, denoted by ϕ , was used as the performance measure [11]. The computation time T (in secs) of each method running in a computer equipped with 2.80-GHz Core i7-930 CPU and 12GB memory is used as the complexity measure. Table 2 shows the average ϕ (degrees) and average T (secs) per realization over various algorithms. Herein, the boldface value denotes the best performance among the tested algorithms for a specific SNR or L . For Case I ($M = 224$, $N = 8$ and $L = 1000$), the performance of all the algorithms improves as the SNR goes up. For Case II ($M = 224$, $N = 8$, SNR = 15 (dB)), the computation time of all the methods increases as L increases. For both cases, the performance of SVMAX, and the computational efficiency of AVMAX and SVMAX are better than that of all the other methods.

In conclusion, we have provided an alternative, continuous optimization-based, perspective on Winter's endmember extraction approach. We have studied a fundamental characteristic of the Winter formulation, and have developed algorithms based on alternating and successive optimization strategies. Remarkably, these algorithms show connections to some existing algorithms, namely, SC-N-FINDR and VCA. Thus, our development offers new interpretations to these existing algorithms. The journal version of this paper [13] will describe more implications and results brought about by the continuous optimization perspective.

5. APPENDIX

5.1. Proof of Theorem 1. Sufficiency of Theorem 1 has been proven in [10]. Now, we show the necessity of Theorem 1. Suppose that $\{\nu_1^*, \dots, \nu_N^*\} = \{\alpha_1, \dots, \alpha_N\}$. This means that $\alpha_i \in \text{conv}\{\tilde{\mathbf{x}}[1], \dots, \tilde{\mathbf{x}}[L]\}$ for all i . Since $\{\alpha_1, \dots, \alpha_N\}$ are affinely independent, every α_i cannot be represented by any non-trivial convex combination of $\{\alpha_1, \dots, \alpha_N\}$. Hence, by (2), we must have $\alpha_i = \tilde{\mathbf{x}}[\ell_i]$ for some ℓ_i and for all i ; that is, (A4). ■

5.2. Proof of Lemma 1. By substituting $\nu_j = \tilde{\mathbf{X}}\boldsymbol{\theta}_j$ into the objective function, problem (7) can be equivalently written as

$$\max_{\boldsymbol{\theta}_j \succeq \mathbf{0}, \mathbf{1}_L^T \boldsymbol{\theta}_j = 1} \mathbf{b}_j^T \tilde{\mathbf{X}} \boldsymbol{\theta}_j, \quad (16)$$

Table 1. The two proposed optimization algorithms for handling Winter's problem (3).

The AVMAX Algorithm	The SVMAX Algorithm
<p>Given a convergence tolerance $\varepsilon > 0$, $\{\tilde{\mathbf{x}}[n]\}_{n=1}^L$ and N.</p> <p>S1. randomly select $(\hat{\nu}_1, \dots, \hat{\nu}_N)$ from $\{\tilde{\mathbf{x}}[n]\}_{n=1}^L$.</p> <p>S2. set $j := 1$, $\varrho := \det(\Delta(\hat{\nu}_1, \dots, \hat{\nu}_N))$, and $\kappa = 0$.</p> <p>S3. calculate $\mathbf{b}_j = [(-1)^{i+j} \det(\mathbf{V}_{ij})]_{i=1}^{N-1}$, and update $\hat{\nu}_j := \tilde{\mathbf{x}}[\ell]$ for any $\ell \in \arg \max_n \mathbf{b}_j^T \tilde{\mathbf{x}}[n]$.</p> <p>S4. if $(j \bmod N) \neq 0$, then $j := j + 1$ and go to S3, else update $\kappa := \kappa + 1$, and $\bar{\varrho} = \det(\Delta(\hat{\nu}_1, \dots, \hat{\nu}_N))$.</p> <p>S5. if $\bar{\varrho} - \varrho /\varrho > \varepsilon$, then set $\varrho := \bar{\varrho}$, $j := 1$, and go to S3, else output $(\hat{\nu}_1, \dots, \hat{\nu}_N)$ as an approximate solution to (3).</p>	<p>Given $\{\tilde{\mathbf{x}}[n]\}_{n=1}^L$ and N.</p> <p>S1. construct $\tilde{\mathbf{x}}[n] = [\tilde{\mathbf{x}}[n]^T \mathbf{1}]^T$ for all n, and set $j = 1$.</p> <p>S2. obtain $\hat{\nu}_1 = \tilde{\mathbf{x}}[\ell]$ for any $\ell \in \arg \max_n \ \tilde{\mathbf{x}}[n]\ _2$, and set $\widehat{\mathbf{W}} = \tilde{\mathbf{x}}[\ell]$.</p> <p>S3. update $j := j + 1$ and obtain $\hat{\nu}_j = \tilde{\mathbf{x}}[\ell]$ for any $\ell \in \arg \max_n \ \mathbf{P}_{\widehat{\mathbf{W}}}^{\perp} \tilde{\mathbf{x}}[n]\ _2$.</p> <p>S4. update $\widehat{\mathbf{W}} := [\widehat{\mathbf{W}} \tilde{\mathbf{x}}[\ell]] \in \mathbb{R}^{N \times j}$ and go to S3 until $j = N$.</p> <p>S5. output $(\hat{\nu}_1, \dots, \hat{\nu}_N)$ as an approximate solution to (3).</p>

Table 2. Performance comparison of average root-mean-square spectral angle distance ϕ (degrees) and average computation time T (secs) per realization over various endmember extraction methods.

Algorithms		Case I: $M = 224, N = 8, L = 1000$						Case II: $M = 224, N = 8, \text{SNR} = 15 \text{ (dB)}$					
		SNR (dB)						L					
		5	15	25	35	45	∞	2000	4000	8000	16000	32000	64000
VCA	ϕ	15.34	3.79	1.26	0.44	0.13	0	3.45	3.43	3.66	3.49	3.68	3.58
	T	0.12	0.08	0.08	0.06	0.05	0.03	0.05	0.07	0.11	0.22	0.48	0.95
SQ-N-FINDR	ϕ	14.17	3.49	1.08	0.32	0.10	0	3.19	3.11	3.11	3.12	3.20	3.34
	T	0.19	0.15	0.13	0.12	0.12	0.12	0.25	0.50	1.01	2.27	4.74	10.00
SC-N-FINDR	ϕ	14.59	3.74	1.18	0.32	0.11	0	3.49	3.41	3.56	3.50	3.78	3.72
	T	0.08	0.07	0.06	0.06	0.06	0.06	0.10	0.19	0.38	0.87	1.86	3.78
AVMAX	ϕ	15.00	3.55	1.07	0.32	0.10	0	3.21	3.09	3.09	3.13	3.33	3.38
	T	0.05	0.04	0.03	0.03	0.03	0.02	0.03	0.04	0.07	0.16	0.39	0.77
SVMAX	ϕ	15.03	3.33	0.94	0.28	0.09	0	3.07	2.94	2.95	3.03	3.10	3.10
	T	0.04	0.03	0.03	0.03	0.03	0.02	0.02	0.04	0.07	0.16	0.39	0.79

where the term $(-1)^{N+j} \det(\mathbf{V}_{Nj})$ in (7) is removed without change of optimality. By letting $\theta_{jn} = [\theta_j]_n$, we have

$$\mathbf{b}_j^T \tilde{\mathbf{X}} \boldsymbol{\theta}_j = \sum_{n=1}^L \theta_{jn} \mathbf{b}_j^T \tilde{\mathbf{x}}[n] \leq \max_{n=1, \dots, L} \mathbf{b}_j^T \tilde{\mathbf{x}}[n] \quad (17)$$

for any $\boldsymbol{\theta}_j \succeq \mathbf{0}$ and $\mathbf{1}_L^T \boldsymbol{\theta}_j = 1$. Moreover, it can be verified that the equality in (17) holds if and only if $\sum_{n \in \mathcal{I}_j} \theta_{jn} = 1$ for \mathcal{I}_j given by (8). Hence, the solution of (16), $\hat{\nu}_j$, can be any convex combinations of $\tilde{\mathbf{x}}[\ell]$ for all $\ell \in \mathcal{I}_j$. ■

5.3. Proof of Lemma 3. Consider (14). By substituting $\mathbf{w}_1 = \tilde{\mathbf{X}} \boldsymbol{\theta}$ into the objective function of (14) for $j = 1$ and by triangle inequality, we have

$$\max_{\substack{\boldsymbol{\theta} \succeq \mathbf{0} \\ \mathbf{1}_L^T \boldsymbol{\theta} = 1}} \left\| \sum_{n=1}^L \theta_n \tilde{\mathbf{x}}[n] \right\|_2 \leq \max_{\substack{\boldsymbol{\theta} \succeq \mathbf{0} \\ \mathbf{1}_L^T \boldsymbol{\theta} = 1}} \sum_{n=1}^L \theta_n \|\tilde{\mathbf{x}}[n]\|_2 \leq \max_n \|\tilde{\mathbf{x}}[n]\|_2. \quad (18)$$

It can be easily verified that the equality above is achieved if and only if $\boldsymbol{\theta} = \mathbf{e}_\ell$ for any $\ell \in \arg \max_{n=1, \dots, L} \|\tilde{\mathbf{x}}[n]\|_2$. Hence, the solution $\hat{\mathbf{w}}_1 = \tilde{\mathbf{x}}[\ell]$ is arrived. The proof for (14) when $j > 1$ is the same as above, and hence is omitted for brevity. ■

6. REFERENCES

- [1] B. A. Campbell, *Radar Remote Sensing of Planetary Surfaces*, New York: Cambridge University Press, 2002.
- [2] N. Keshava and J. Mustard, "Spectral unmixing," *IEEE Signal Process. Mag.*, vol. 19, no. 1, pp. 44–57, Jan. 2002.
- [3] J. M. Bioucas-Dias and A. Plaza, "Hyperspectral unmixing: Geometrical, statistical, and sparse regression-based approaches," in *Proc. of SPIE - Image and Signal Processing for Remote Sensing XVI*, Toulouse, France, Sept. 20, 2010, vol. 7830.
- [4] L. Miao and H. Qi, "Endmember extraction from highly mixed data using minimum volume constrained nonnegative matrix factorization," *IEEE Trans. Geosci. Remote Sens.*, vol. 45, no. 3, pp. 765–777, Mar. 2007.
- [5] J. M. B. Dias, "A variable splitting augmented Lagrangian approach to linear spectral unmixing," in *Proc. First IEEE Workshop on Hyperspectral Image and Signal Processing: Evolution in Remote Sensing (WHISPERS)*, Grenoble, France, Aug. 26–28, 2009.
- [6] T.-H. Chan, C.-Y. Chi, Y.-M. Huang, and W.-K. Ma, "A convex analysis based minimum-volume enclosing simplex algorithm for hyperspectral unmixing," *IEEE Trans. Signal Process.*, vol. 57, no. 11, pp. 4418–4432, Nov. 2009.
- [7] M. D. Craig, "Minimum-volume transforms for remotely sensed data," *IEEE Trans. Geosci. Remote Sens.*, vol. 32, no. 3, pp. 542–552, May 1994.
- [8] M. E. Winter, "N-findr: An algorithm for fast autonomous spectral end-member determination in hyperspectral data," in *Proc. SPIE Conf. Imaging Spectrometry*, Pasadena, CA, Oct. 1999, pp. 266–275.
- [9] C.-C. Wu, S. Chu, and C.-I. Chang, "Sequential N-FINDR algorithms," *Proc. of SPIE*, vol. 7086, Aug. 2008.
- [10] T.-H. Chan, W.-K. Ma, C.-Y. Chi, and A. Ambikapathi, "Hyperspectral unmixing from a convex analysis and optimization perspective," in *Proc. First IEEE WHISPERS*, Grenoble, France, August 26–28, 2009.
- [11] J. M. P. Nascimento and J. M. B. Dias, "Vertex component analysis: A fast algorithm to unmix hyperspectral data," *IEEE Trans. Geosci. Remote Sens.*, vol. 43, no. 4, pp. 898–910, Apr. 2005.
- [12] D. P. Bertsekas, *Nonlinear Programming*, MA: Athena Scientific, 1999.
- [13] T.-H. Chan, W.-K. Ma, A. Ambikapathi, and C.-Y. Chi, "A simplex volume maximization framework for hyperspectral endmember extraction," to appear in *IEEE Trans. on Geoscience and Remote Sensing— Special Issue on Spectral Unmixing of Remotely Sensed Data*, 2011.